Nuclear magnetic resonance lineshape studies of interpenetrating polymer networks

Nathalie Parizel*, Guy Meyer and Gilbert Weill
Institut Charles Sadron (CRM-EAHP), CNRS-ULP Strasbourg, 6 rue Boussingault, 67083 Strasbourg Cedex, France
(Received 21 April 1992; revised 20 July 1992)

In the so-called *in situ* sequential interpenetrating polymer networks (IPNs), the two networks are formed after each other, and the network formed first is thought to impede gross phase separation in the final material. This is contrary to the other type of IPNs (*in situ* simultaneous), in which the formation of both networks is initiated at once and proceeds to completion more or less simultaneously. In order to verify more accurately this assumption, which is not inconsistent with transmission electron microscopy findings, a solid-state nuclear magnetic resonance lineshape analysis technique has been used to investigate the degree of phase dispersion of IPNs of both types composed of an elastomeric polyurethane (PUR) (25 wt%) and a crosslinked poly(methyl methacrylate). The results confirm that such IPNs, when prepared sequentially, have a higher degree of phase dispersion than those obtained by the simultaneous synthesis method. Furthermore, in the corresponding neat PUR networks, built up from aromatic pluriisocyanate and poly(oxypropylene glycol) (POPG), the rigid crosslink points are not composed of isocyanate only, but include some oxypropylene mers; it appears that the amount of the rigidified part is the same, whatever the molecular weight of POPG.

(Keywords: nuclear magnetic resonance; lineshape; interpenetrating polymer networks; poly(methyl methacrylate); polyurethane; *in situ* sequential interpenetrating networks; *in situ* simultaneous interpenetrating networks)

INTRODUCTION

Interpenetrating polymer networks (IPNs) represent a quite original approach to polymer blending[1–3]. As the only way to combine two polymers in the form of their networks, they exhibit limited phase separation, compared to mechanical blends or copolymers[4]. Their structure is in some way frozen as soon as both networks have been formed; except in the case of chemical degradation, stresses will not induce gross topological change in the morphology of an IPN, and therefore in its properties. Another advantage of IPNs is that the method and the conditions of their synthesis can be varied widely, so that, even without changing the composition, very different morphologies[5], and hence properties, may be obtained.

However, IPNs, as intimate associations of two networks, are quite complicated systems, and, owing to their thermoset character, only a few of the usual investigation methods for polymers are suitable for their study. As a consequence, general structure–property relationships have not yet been established, and only their synthesis and some application-oriented properties are usually reported in the literature[6]. Concerning the phase structure of IPNs, a large number of experimental investigations have made use of dynamic mechanical analysis, differential scanning calorimetry, scattering techniques and electron microscopy. Only a few investigations have utilized nuclear magnetic resonance (n.m.r.) to provide morphological characterization of a more detailed nature in networks[7–9] and IPNs[10–13].

^{1}H n.m.r. in the solid state can monitor mobility through either the lineshape (or free induction decay, f.i.d., in the time domain) or the longitudinal relaxation. In a phase-separated system, there should be a temperature range between the glass transition temperature of the two pure components, where the f.i.d. is the superposition of the fast decay arising from the glassy constituent of low mobility and the slow decay arising from the elastomeric constituent of higher mobility. Deviation of the observed f.i.d. from this superposition implies some mixing between the two components. Similarly the longitudinal relaxation is expected to be a superposition of two exponential decays with the T_1 values of the pure components, except for the case where the size of the phases is small enough for the relaxation of the magnetization of the phase with the longer T_1 to occur through spin diffusion to the other phase. This technique has been widely used for the characterization of the crystalline and amorphous phases in semicrystalline homopolymers[14]. We attempt to use it in IPNs based on an elastomeric polyether–polyurethane (PUR) and a crosslinked poly(methyl methacrylate) (PAc). In this case, however, the problem is complicated by the fact that the f.i.d. of the glassy PMMA polymer itself has a composite shape, arising from the methyl rotation, and the elastomeric PUR component also has a composite shape, arising from the existence of 'soft' chains and 'rigid' crosslinks. We therefore have to refine the

* To whom correspondence should be addressed

0032-3861/93/122495-08

Table 1 Raw materials

Material	Description	Supplier
Desmodur L75	1,1,1-Trimethylolpropane/toluene diisocyanate adduct containing 25% ethyl acetate by weight; density, 1.17 g ml^{-1}; 3.06 NCO/kg	Bayer AG
POPG 400	Poly(oxypropylene glycol), $\bar{M}_n$ = 460 g mol^{-1}; density, 1.01 g ml^{-1}; hydroxyl content, 5.20 mol kg^{-1}	Arco Chemicals
POPG 1000	Poly(oxypropylene glycol), $\bar{M}_n$ = 975 g mol^{-1}; density, 1.01 g ml^{-1}; hydroxyl content, 2.14 mol kg^{-1}	Arco Chemicals
POPG 2000	Poly(oxypropylene glycol), $\bar{M}_n$ = 1990 g mol^{-1}; density, 1.0 g ml^{-1}; hydroxyl content, 1.06 mol kg^{-1}	Arco Chemicals
Kosmos 29	Stannous octoate, stabilized; tin content, 29.1% by weight; density, 1.25 g ml^{-1}	Goldschmidt
MMA	Methyl methacrylate; inhibitor, 15 ppm methylethylhydroquinone	Merck
TRIM	1,1,1-Trimethylolpropane trimethacrylate; inhibitor, 100 ppm methylethylhydroquinone	Degussa
AIBN	2,2′-Azobisisobutyronitrile	Merck

comparison of the f.i.d. of the IPN with that of the pure PMMA and PUR networks. We describe here the results obtained on these pure networks and on two IPNs of the same composition but prepared by sequential or simultaneous synthesis.

EXPERIMENTAL

Materials

The raw materials and their description are listed in *Table 1*. The poly(oxypropylene glycol)s (POPG) and the methacrylic monomers were dried by molecular sieves but not otherwise purified. Other materials were used as received.

Synthesis of the individual networks

The polyurethane network was formed at room temperature by reacting Desmodur L75 with POPG under stoichiometric conditions, such as $K = [NCO]/[OH] = 1.07$. Stannous octoate was added last, as its catalytic action begins immediately upon contact with the polyurethane precursors. The mixture was introduced into a mould consisting of two glass plates separated by a 3 mm thick gasket, and allowed to react. The amount of catalyst, typically 0.2–1.0% by weight, was taken to make gelation occur within about 6 h, depending on the molecular weight of the POPG. The rigid network was obtained in bulk by radical copolymerization of methyl methacrylate with 5 wt% TRIM in the presence of 1 wt% AIBN as initiator. Like for polyurethane, the mixture was transferred into a glass mould, heated at 333 K and allowed to polymerize for 2 h. After removal from the mould, the individual networks were annealed at 348 K under vacuum for one night.

Synthesis of IPNs

The IPNs synthesized for this study, containing 25% by weight of polyurethane, were prepared by the *in situ* procedure[15] developed in our laboratory. The reagents, Desmodur L75, POPG, MMA, TRIM and AIBN, were mixed together and poured into a glass mould after addition of stannous octoate. Two different IPNs were made. The first IPN, called *in situ* sequential, was made by keeping the mould at room temperature and in the absence of light up to gelation of the polyurethane and then transferring it to an oven at 333 K. The second IPN, called *in situ* simultaneous, was obtained by heating the mixture at 333 K immediately after filling up the mould. Owing to the different reactivity of stannous octoate at room temperature and at 333 K, the amount of catalyst was 1 wt% and 0.25 wt% for the *in situ* sequential IPN and for the *in situ* simultaneous IPN, respectively. The IPNs were annealed in the same way as the individual networks.

Measurements

The kinetics of IPN formation was followed by Fourier-transform infra-red spectroscopy on a Nicolet 60SX spectrophotometer equipped with a Specac heating chamber. Dynamic mechanical measurements were performed with a Rheometrics mechanical spectrometer at a fixed frequency of 0.16 Hz. The morphology of IPNs was investigated by a Zeiss EM 902 electron microscope equipped with an integrated electron energy-loss spectrometer.

N.m.r. measurements have been carried out on a Bruker SXP spectrometer operating at 60 MHz (^{1}H). The resonance field is monitored with a field frequency lock (Drush, n.m.r. gaussmeter and regulation unit TAO2) within 2 μT. The free induction decay (f.i.d.) signal, following a $\pi/2$ pulse of 4 μs generated by a Hewlett-Packard pattern generator 8175A, is digitized with a LeCroy 6810 with 12 bits (accuracy 1/2000) at the fastest sampling rate of 5 MHz, and finally averaged and treated on an IBM-PC compatible ACER 1100. Numerical computations are performed in Asyst language.

The f.i.d. can be fitted with linear combination of functions of the shape:

$$f(t) = A \exp[-(1/b)(t/T_2)^b] \qquad \text{with } 1 < b < 2$$

Here $b = 1$ corresponds to the case of highly mobile quasi-liquid components; $b = 2$ corresponds to the case of a rigid component with a large number of dipolar coupled protons. For $b = 2$ there is a simple relation between T_2 and the second moment, M_2, of the line, $M_2 = (1/\gamma T_2)^2$. Intermediate values of b can be explained by entanglements[16].

A superposition of Gaussian and exponential functions has generally been found suitable to simulate the f.i.d.[17]. Extrapolation of the signal to the middle of the pulse ($t = 0$) through the dead time of the receiver (5 μs) provides the relative amount of each component. Up to three components (seven parameters) are adjusted by non-linear least-squares fits.

Measurements of the hydrogen spin–lattice relaxation times T_1 at 60 MHz have been performed between 213 and 423 K on PMMA and PUR homonetworks by the so-called inversion–recovery sequence. Within experimental accuracy, the relaxation is monoexponential.

Table 2 T_1 *versus* temperature for PAc and PUR homonetworks

	T_1 (ms)	
Temperature (K)	PAc	PUR ($M_{n,POPG} = 1990\ g\ mol^{-1}$)
213	240	280
273	180	240
303	170	140
343	230	160
393	360	260
423	420	480

Table 3 Free induction decay (f.i.d.) decomposition of the poly(methyl methacrylate) network

	Rigid component		Mobile component	
Temperature (K)	^{1}H (%)	M_2 or T_2	^{1}H (%)	M_2 or T_2
116	62.5	16.0 G^2	37.5	5.4 G^2
298	61.5	13.5 G^2	38.5	20 μs
323	61.5	13.5 G^2	38.5	20 μs
343	61.5	13.5 G^2	38.5	22 μs
363	61.0	13.0 G^2	39.0	23 μs
383	61.0	12.0 G^2	39.0	25 μs
403	61.0	10.0 G^2	39.0	37 μs
423	54.5	7.0 G^2	45.5	54 μs
443	53.0	3.0 G^2	47.0	133 μs
463	52.0	70 μs	48.0	500 μs

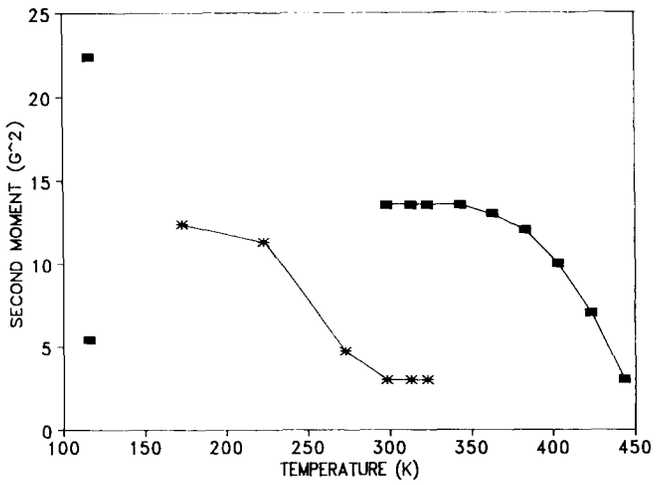

Figure 1 Second Moment M_2 (G^2) *versus* temperature T(K) of the PAc and PUR homonetworks: (■) PAc, (*) PUR

RESULTS AND DISCUSSION

Poly(methyl methacrylate) network

The rigid methacrylic network (PAc) results from radical copolymerization, hence giving a random distribution of crosslink points. An accumulation of TRIM, which is the crosslinker, along the chain has not been reported, and regions of enhanced rigidity due to a higher local crosslink density are therefore of low probability. Dynamic mechanical analysis of the PAc network shows a broad β transition centred around 273 K and a maximum at 403 K corresponding to the glass transition temperature, in close analogy to linear PMMA[18].

The values of the spin–lattice relaxation times T_1 *versus* temperature are reported in *Table 2* and will be compared later to those of the PUR homonetwork. The minimum around 303 K indicates correlation times of about 5 ns corresponding to the β transition.

Between 298 and 443 K the f.i.d. are well fitted by the superposition of a Gaussian and an exponential. Their relative fractions, second moment and T_2 are given in *Table 3* and *Figures 1* and *2*. One experiment has been carried out at 116 K and analysed by the superposition of an Abragam function and one Gaussian function (*Figure 3*):

$$g(t) = A_1 \exp[-0.5(at)^2] \sin(bt)/bt + A_2 \exp[-0.5(t/T_2)^2]$$

From the relative fractions $A_1 = 62\%$ and $A_2 = 38\%$ one can:

(i) compute the total second moment:

$$M_{2tot} = [(0.62 \times 22.4) + (0.38 \times 5.4)] = 16\ G^2$$

which fits the value calculated from the PMMA structure with one rotating methyl[19];

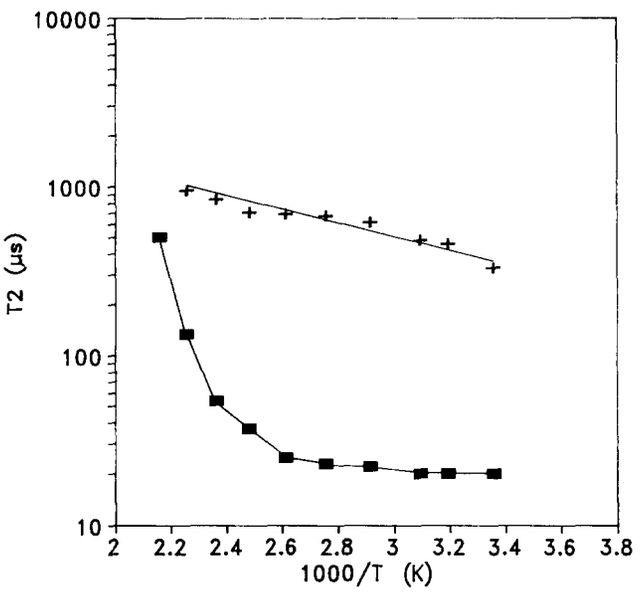

Figure 2 Logarithm of T_2 (μs) *versus* 1000/T(K) for the PAc and PUR homonetworks: (■) PAc, (+) PUR

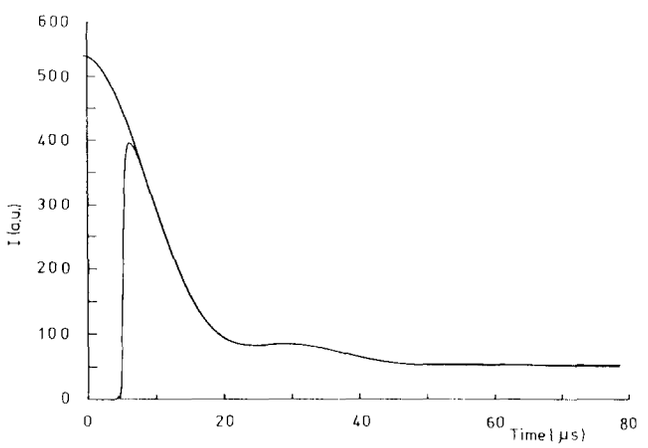

Figure 3 Experimental f.i.d. and best-fitted curve for the PAc homonetwork at 116 K with:

$$g(t) = A_1 \exp[-0.5(at)^2] \sin(bt)/bt + A_2 \exp[-0.5(t/T_2)^2]$$

where $A_1 = 0.62$; $A_2 = 0.38$; $a = 4.76 \times 10^4\ s^{-1}$; $b = 2.08 \times 10^5\ s^{-1}$; $T_2 = 1.61 \times 10^{-5}$ s

Table 4 Glass transition temperature T_g and f.i.d. decomposition of various PUR networks at 300 K

		Component I			Component II			Component III		
$\bar{M}_{n,POPG}$ (g mol^{-1})	T_g (K)	^{1}H (%)	T_2 (μs)	b	^{1}H (%)	T_2 (μs)	b	^{1}H (%)	T_2 (μs)	b
460	264	67	20	1.6	21	90	1	12	600	1
975	253	36	20	1.6	48	100	1	16	260	1
1990	237	21	20	1.6				79	330	1.2

(ii) observe that the value of $M_2 = 5.4\ G^2$ is very close to that expected for an isolated CH_3 group rotating around its C_3 axis (22/4)[20]; and

(iii) deduce that the values $A_2 \simeq 3/8$ and $M_2 \simeq 5\ G^2$ suggest that the rotating methyl is very weakly coupled to the other protons of the chain and behaves like a 'mobile region' of the polymer.

The latter would imply that it corresponds to the methyl ester. This is in agreement with the work of Jelinski[21]. The similarity in the fractions of Gaussian and exponential decay, and the lower value of M_2 ($\simeq 13.5\ G^2$) observed in the range 268–363 K suggest that the α methyl is now also rotating in good agreement with previous values of the total second moment[19,22–25], while the methyl ester has a quasi-isotropic motion above the temperature of the β transition. The further decrease of M_2 and increase of T_2 over 403 K indicate the onset of the glass transition. The rather high value of T_g is due both to the frequency of observation (the inverse of the linewidth) and to the crosslinking of the PMMA network. The sample becomes liquid-like at 463 K.

The fit of the f.i.d. between 116 and 296 K as a superposition of an Abragam and a Gaussian or two Gaussians or one Gaussian and an exponential with $A_1 = 5/8$ and $A_2 = 3/8$ is not satisfactory.

Polyurethane networks

These elastomeric networks are made from a pluriisocyanate and a poly(oxypropylene glycol) (POPG) without the addition of any chain extender. Such a polyaddition reaction yields constant chain lengths between crosslinks, and by varying the molecular weight of POPG, the elastomeric behaviour of the network is affected. The glass transition temperatures of the polyurethane networks appear in *Table 4* for three POPG of different molecular weights.

All these networks are densely crosslinked as the elastic chains are rather short ($\bar{M}_{n,POPG}$ from 460 to 1990 g mol^{-1}). Their characterization has been reported in detail by Tabka *et al.*[26]: the structure depends on the dilution of the polyurethane precursors in the reaction medium, and on the number of isocyanate functions per hydroxy function. In the IPNs examined here, both dilution (25 wt% in methacrylic monomers) and the stoichiometric ratio ($K = [NCO]/[OH] = 1.07$) have been set to give networks with least defects, i.e. dangling or loose POPG chains. However, within these limits, more defects always arise with the lowest $\bar{M}_n$. The presence of hydrogen bonds between urethane mers or between urethane and POPG is likely, and contributes to rigidify locally the polyurethane network, whereas network defects should have the reverse effect.

The values of the spin–lattice relaxation times T_1 *versus* temperature are reported in *Table 2* for a PUR ($\bar{M}_{n,POPG} = 1990$ g mol^{-1}). In the range of temperature examined, the two homonetworks exhibit similar T_1 values and therefore no information on phase separation can be expected from the measurement of T_1 in the IPNs.

The decomposition of the f.i.d. of the PUR network at different temperatures is reported in *Table 5*, and the variations of M_2 and $\log(T_2)$ in *Figures 1* and *2*. At the lowest temperatures, the f.i.d. is well represented by a Gaussian curve, with $M_2 = 12.4\ G^2$ at 173 K and $M_2 = 11.3\ G^2$ at 223 K; these values correspond to a relaxation time T_2 of approximately 10 μs and indicate that the PUR network is totally rigid. From 273 K, the f.i.d. can be fitted by the superposition of a Gaussian decay and an exponential decay, the latter corresponding to a fraction of over 75%. It should be noted that the glass transition temperature of the PUR network is located between the two latter temperatures. The amount of mobile part as well as the T_2 value increase with temperature. From 343 K upwards, the f.i.d. can be fitted by a single exponential with a T_2 reaching 950 μs at 443 K.

The variation of f.i.d. with the chain length of POPG has also been examined. At 300 K, the decomposition of the f.i.d. is given in *Table 4*. Owing to a ratio of at least three for the time constants, the fractions deduced from the f.i.d. can be considered as significant.

In the case of PUR with POPG 1000, the relaxation of the mobile part has been taken as a sum of two exponentials. For the PUR with POPG 2000, the b exponent is 1.2 instead of 1, owing to entanglements, and the value of T_2 is shifted to the even higher value of 330 μs. The fact that the PUR with the lowest elastic chain length has a high T_2 of 600 μs may be attributed to the non-negligible amount of dangling chains present in such a network.

In a first approach, the crosslinker molecule (i.e. L75) and the POPG can be considered, respectively, as the rigid and as the mobile part of the PUR network. In order to verify this assumption, the rigid ^{1}H fraction (the ratio of ^{1}H belonging to L75 to the total number of ^{1}H) has been calculated from the composition of the reaction mixture and compared to the value given by the f.i.d.

The number of hydrogen atoms per spacer branch has been deduced from the formula of POPG:

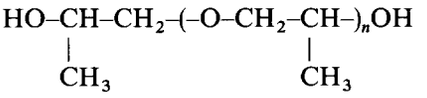

Table 5 F.i.d. decomposition of the PUR network ($\bar{M}_{n,POPG}$ = 1990 g mol^{-1})

	Rigid component			Mobile component		
Temperature (K)	^{1}H (%)	M_2 or T_2	b	^{1}H (%)	T_2 (μs)	b
173	100	12.4 G^2	2			
223	100	11.3 G^2	2			
273	23.7	4.7 G^2	2	76.3	120	1
298	21.3	20 μs	1.6	78.7	330	1.2
313	12.5	20 μs	1.6	87.5	460	1.2
323	11.2	20 μs	1.6	88.8	480	1.2
343				100	620	1.2
363				100	670	1.2
383				100	690	1.3
403				100	710	1.5
423				100	840	1.5
443				100	950	1.5

Table 6 Number of ^1H in the various PURs and their precursors

$\bar{M}_{n,POPG}$ (g mol^{-1})	Number of mers	Number of ^1H in POPG	Number of ^1H in L75
460	6	44	23
975	16	104	23
1990	33	206	23

Table 7 Calculated and experimental amounts of rigid ^1H in the PUR networks

$\bar{M}_{n,POPG}$ (g mol^{-1})	Amount (%) of rigid ^1H		Number of rigidified ^1H from POPG
	Calculated	Experimental	
460	34.3	67	22
975	18.1	36	23
1990	10.0	21	25

For a molecular weight of 751, there are 31 ^1H in the L75. The correct weight and the number of ^1H associated with L75 have been obtained through the relation between the amounts of L75 and POPG used to form the PUR network (see *Table 1*).

The different values are given in *Table 6*. The comparison of the number of rigid ^1H belonging to L75 with the experimental f.i.d. values (*Table 7*) clearly shows a greater fraction of immobilized hydrogen atoms than expected from only the isocyanate contribution. This result leads one to assume that some segments of the POPG chain near the crosslink points have restricted mobility, and the number of oxypropylene monomer units UR that are involved in this rigidification has been determined:

$$f_{rigid} = (N_{L75} + xN_{POPG})/N_e$$

where x is the fraction of rigid ^1H from oxypropylene glycol and N_e the total number of ^1H. Then,

$$xN_{POPG} = N_e(f_{exp}) - N_{L75}$$

where f_{exp} is the experimental ratio determined from the f.i.d. This relation gives the number of rigid ^1H belonging to the POPG chain (*Table 7*), which is nearly the same for all the samples, and allows to determine a value for UR near 3.

Polyurethane/poly(methyl methacrylate) IPNs

Two IPN samples, both containing 25% polyurethane by weight ($\bar{M}_{n,POPG} = 1990$ g mol^{-1}), have been examined. One has been obtained by the *in situ* sequential mode (seqIPN), the other by the *in situ* simultaneous mode (simIPN). The difference in kinetics imparted to the synthesis process appears in *Figure 4*. For the seqIPN, the polyurethane network is almost completely formed before the onset of radical copolymerization. Hence, the methacrylic monomers are finely dispersed in the polyurethane matrix, and owing to the highly viscous reaction medium, which makes termination by diffusion rather difficult, polymerization is likely to go to complete conversion[27]. The simIPNs are formed in a different way: both reactions, polyaddition and radical polymerization, start at once but proceed with different kinetics. In the present experimental conditions, the polymethacrylic network is formed prior to the polyurethane one, and consequently, owing to the rigid nature of the PAc network, the polyurethane network is imperfectly formed. It may be anticipated that the degree of mixing is the greatest for the seqIPN, whereas gross phase separation takes place for the simIPN, and in fact such a situation is revealed by electron microscopy (*Figure 5*). Definitely different morphologies may hence be obtained by varying only one parameter of synthesis. The transition behaviour also reflects these results: the simIPN shows two transitions close to those of the individual networks, whereas the seqIPN shows broadened and damped transitions shifted inwards compared to those of the neat networks[5].

The experimental results of the f.i.d. decomposition into three components for the simIPN and for the seqIPN are given in *Tables 8* and *9* respectively. According to previous results for the individual networks, the first rapid decay is similar to the one of rigid PAc, and the slowest one to that of mobile PUR. In the intermediate region,

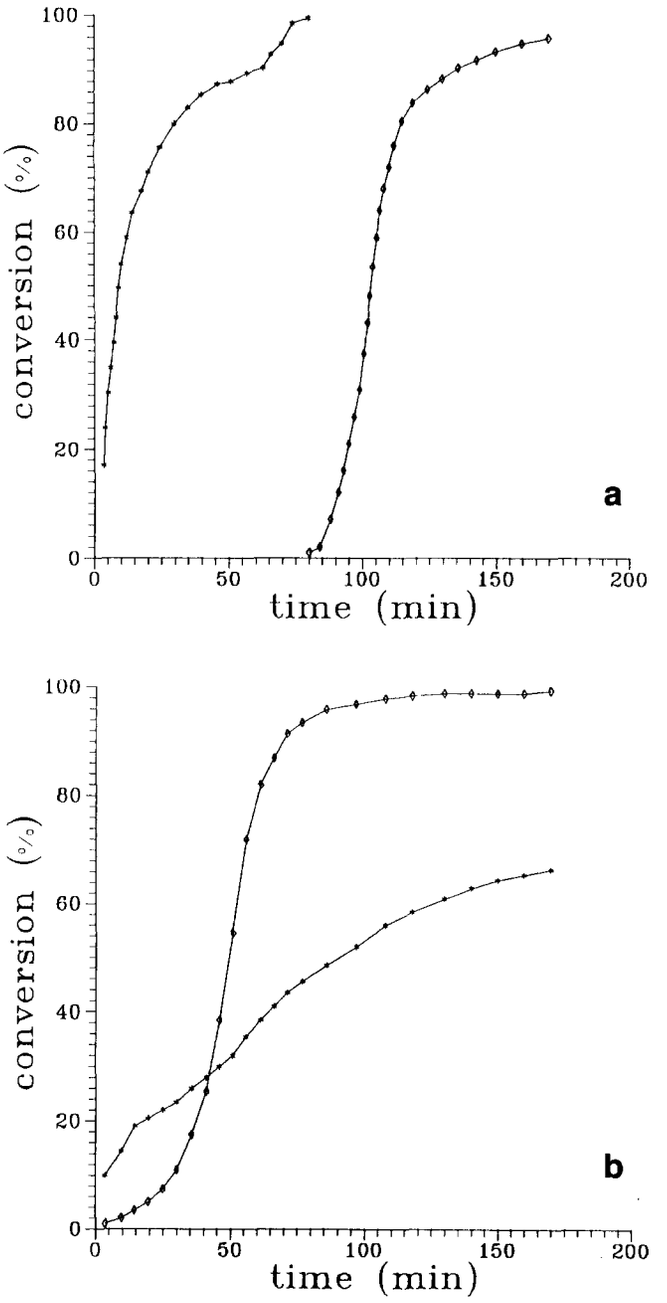

Figure 4 Percentage of conversion *versus* time (min) for (a) seqIPN and (b) simIPN: (*) PUR, (◆) PAc

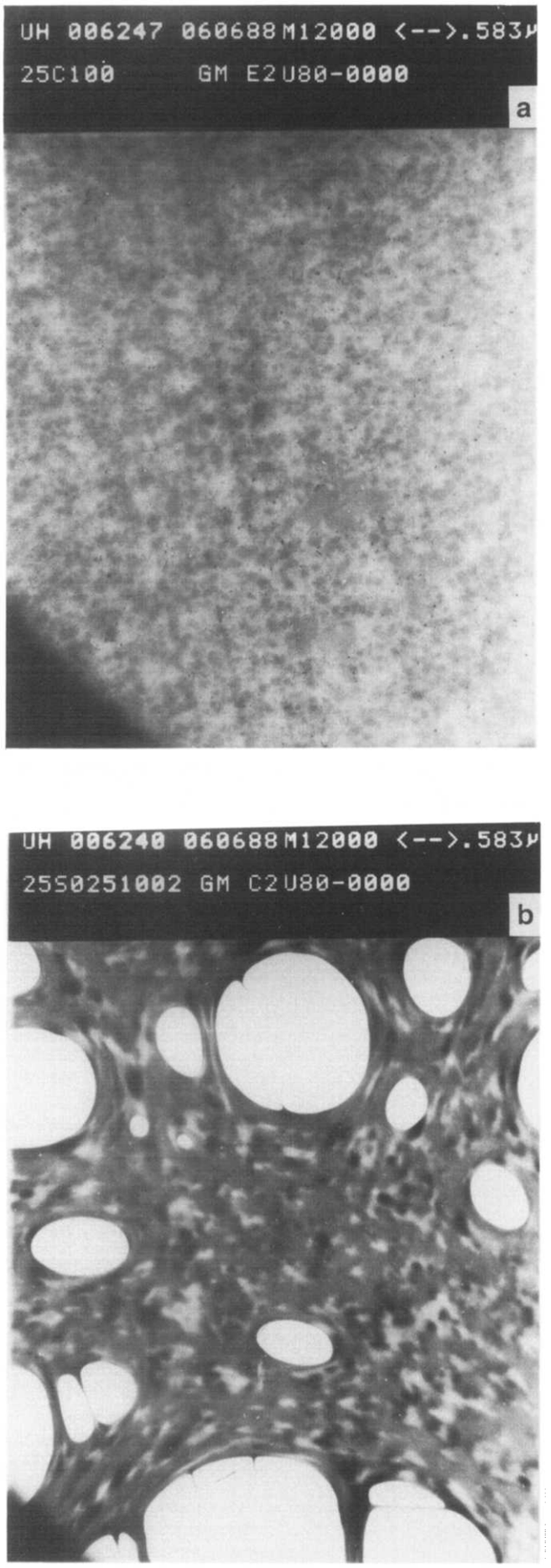

Figure 5 Transmission electron micrographs of (a) seqIPN and (b) simIPN

both mobile PAc and rigid PUR contribute to the lineshape. It has been assumed that the signals from the IPN are linear combinations of the two networks, and the f.i.d. has been calculated by such a linear combination of the mobile and rigid zones of PUR and PAc with respectively 27.5% and 72.5% representing the percentages of associated ^1H. The calculated f.i.d. have then been analysed in the same way as the recorded ones. The results are given in *Table 10*: the decay of the rigid part of PUR between 298 and 323 K ($M_2 = 3\,G^2$) is not distinct from the decay due to the methyl ester of PAc ($T_2 = 20\,\mu s$). Hence, three components may be distinguished in the IPN f.i.d.: a rigid part representative of PAc, an intermediate region to which both PAc and PUR contribute, and the tail of the signal due only to the PUR network.

In *Figures 6* and *7*, the variations of the amounts of observed rigid and mobile components are compared with the calculated ones as a function of temperature. Below 323 K, the magnitude of the more rapid decay is greater and the tail less important than expected by

Table 8 Experimental f.i.d. decomposition of the simIPN

	Rigid component		Intermediate		Mobile component	
Temperature (K)	^1H (%)	M_2 (G^2)	^1H (%)	T_2 (μs)	^1H (%)	T_2 (μs)
298	49.1	13	32.5	22	18.4	300
323	47.4	13	30.9	22	21.7	460
343	40.6	13	35.7	20	23.7	620
363	41.3	12.8	32.7	21.5	26.0	590
383	40.0	12.2	31.5	23	28.5	610
403	31.6	11.1	33.8	24	31.6	640
423	29.0	8.8	35.1	28	35.9	660
443	16.9	6.5	41.0	32	42.1	590

Table 9 Experimental f.i.d. decomposition of the seqIPN

	Rigid component		Intermediate		Mobile component	
Temperature (K)	^1H (%)	M_2 (G^2)	^1H (%)	T_2 (μs)	^1H (%)	T_2 (μs)
298	47.6	12.3	41.0	21	11.4	230
323	44.9	12.6	37.4	23	17.7	410
343	38.3	13.3	40.4	23	21.3	560
363	40.0	12.1	33.6	25	26.4	690
383	27.1	10.4	36.4	26	32.6	680
403	26.9	11.1	40.5	23.4	36.5	805
423	17.5	8	37.7	28	44.8	660
443	1.4	7	45.8	23	52.8	430

Table 10 Calculated f.i.d. decomposition by combination of PUR and PAc decays

	Rigid component		Intermediate		Mobile component	
Temperature (K)	^1H (%)	M_2 (G^2)	^1H (%)	T_2 (μs)	^1H (%)	T_2 (μs)
298	44.6	13.8	33.8	20	21.6	330
323	44.6	13.6	31.0	22	24.4	480
343	44.6	13.5	27.9	22	27.5	620
363	44.2	13	28.3	23	27.5	670
383	44.2	12	28.3	25	27.5	690
403	44.2	10	28.3	38	27.5	710
423	39.5	6.8	33.0	50	27.5	840
443	38.4	3.5	34.1	130	27.5	950

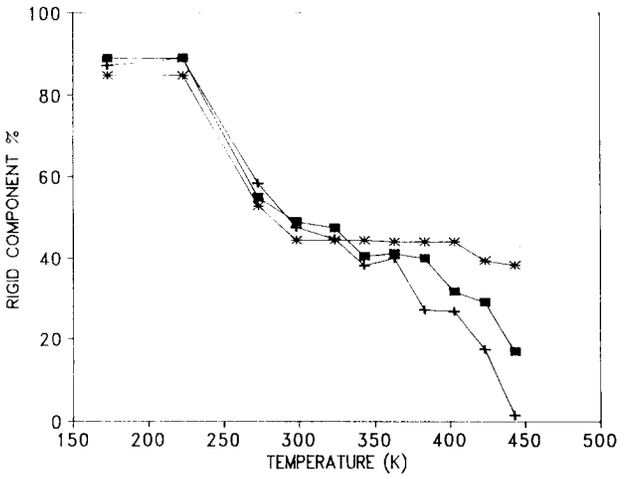

Figure 6 Percentage of rigid component *versus* temperature (K): (+) seqIPN, (■) simIPN, (*) calculated

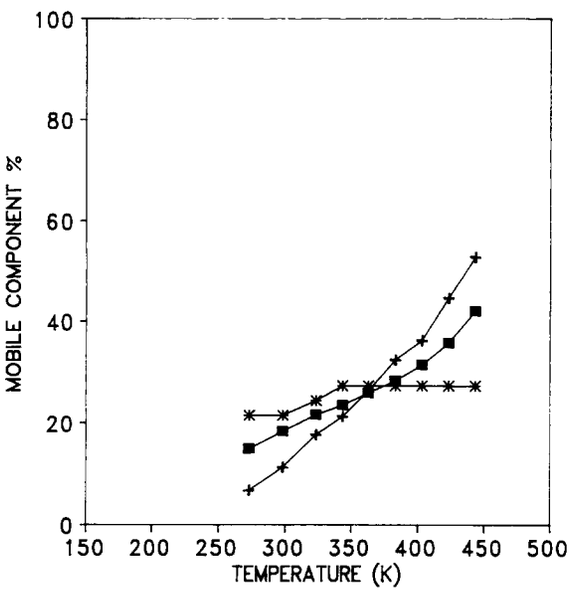

Figure 7 Percentage of mobile component *versus* temperature (K): (+) seqIPN, (■) simIPN, (*) calculated

calculation. As the tail is only representative of PUR, one can conclude that a part of PUR has been rigidified. The decay of this part of the curve occurs either in the intermediate zone or in the more rigid one. By subtraction of the calculated ratios from the experimental ones, it appears that a non-negligible part of PUR, 11% at 298 K, acquires a quite important second moment of $12\,G^2$ instead of $3\,G^2$. The PUR mobility is hindered by the presence of PAc.

Above 363 K, these tendencies are inverted: the Gaussian component is weaker at the beginning, while the tail of the f.i.d. of the IPNs is more important than the corresponding computed signal. As the entire PUR is mobile above 343 K, if the magnitude of the exponential tail represents more than 27.5%, this implies that it comprises a part of PAc hydrogens. Hence, PAc is more mobile in this temperature range when it is in the presence of PUR. This is expressed by a decrease of the rigid component and an increase of the mobile one, while the decrease associated with the CH_3 ester is shifted to the tail of the f.i.d. A possible interpretation of the observed inversion could be the disappearance of any rigid part in PUR around 343 K (*Table 5*). The evolutions of the component intensities are the same for the simIPN and for the seqIPN: below 323 K, the mobility of PUR decreases, and above 363 K, it is the one of PAc which increases. However, these effects are clearly more pronounced in the case of the seqIPN than for the simIPN.

The changes in mobility of the components in the interpenetrated networks, when compared to the individual networks, correspond to interactions between these components. The more drastic changes for the seqIPN indicate stronger interactions between the two components. These experiments allow one to conclude that the PAc and PUR networks are more intimately mixed (in a range of 2–5 Å) after a sequential preparation mode.

CONCLUSION

A noticeable finer phase dispersion is obtained in IPNs synthesized sequentially than in the corresponding simultaneous ones. These results may be explained by the fact that, in the former type of IPN, the PUR host network is completely formed before the onset of copolymerization of the second component: its presence precludes the formation of large rigid domains, contrary to the case where the two networks formed simultaneously possess a morphology with larger domains. The same investigation technique has been applied to neat PUR networks with elastic chains of various lengths: whatever the molecular weight of POPG, an equal amount of oxypropylene mers is rigidified per crosslink point, which therefore does not consist only of isocyanate.

Although this study is a necessary prerequisite, more experiments are needed for quantitative evaluation: in a next step, the molecular proximity of the two components by spin diffusion in the rigid parts will be examined using selective ^{13}C cross-polarization.

REFERENCES

1 Sperling, L. H. 'Interpenetrating Polymer Networks and Related Materials', Plenum Press, New York, 1981
2 Sperling, L. H. in 'Multicomponent Polymer Materials' (Eds D. R. Paul and L. H. Sperling), American Chemical Society, Washington, DC, 1986
3 Frisch, K. C., Klempner, D. and Frisch, H. L. *Polym. Eng. Sci.* 1982, **22**, 1143
4 Huelck, V., Thomas, D. A. and Sperling, L. H. *Macromolecules* 1972, **5**, 340, 348
5 Tabka, M. T., Widmaier, J. M. and Meyer, G. C. in 'Sound and Vibration Damping with Polymers' (Eds R. D. Corsaro and L. H. Sperling), American Chemical Society, Washington, DC, 1990
6 Klempner, D. and Frisch, K. C. 'Advances in Interpenetrating Polymer Networks', Technomic, Lancaster, PA, 1989
7 Douglass, D. C. and McBrierty, V. J. *Polym. Eng. Sci.* 1979, **19**, 1054
8 Assink, R. A. *J. Polym. Sci., Polym. Chem. Edn.* 1977, **15**, 59
9 Guillermo, A., Cohen-Addad, J. P. and Le Nest, J. F. *Macromolecules* 1991, **24**, 3081
10 Lipatov, Yu. S., Chramova, T. S., Sergeeva, L. M. and Karabanova, L. V. *J. Polym. Sci., Polym. Chem. Edn.* 1977, **15**, 427
11 Edbon, J. R., Hourston, D. J. and Klein, P. G. *Polymer* 1986, **27**, 1807
12 McDonald, C. J., Smith, P. B., Roper, J. A., Lee, D. I. and Galloway, J. G. *Colloid Polym. Sci.* 1991, **269**, 227
13 Ku, W. H., Liang, J. L., Wei, K. T., Liu, H. T., Huang, C. S., Fang, S. Y. and Wu, W. G. *Macromolecules* 1991, **24**, 4605

14 Bergmann, Von K. *Kolloid Z. Z. Polym.* 1973, **251**, 962
15 Djomo, H., Morin, A., Damyanidu, M. and Meyer, G. C. *Polymer* 1983, **24**, 65
16 Cohen-Addad, J. P. *J. Physique* 1982, **10**, 1509
17 Hirschinger, J., Meurer, B. and Weill, G. *Polymer* 1987, **28**, 721
18 Albert, B., Jérôme, R., Teyssié, P., Smyth, G., Boyle, N. G. and McBrierty, V. J. *Macromolecules* 1985, **18**, 388
19 Sinnott, K. M. *J. Polym. Sci.* 1960, **42**, 3
20 Gutowsky, H. S. and Pake, G. E. *J. Chem. Phys.* 1950, **18**, 162
21 Jelinski, L. W. *Annu. Rev. Mater. Sci.* 1985, **15**, 359
22 Powles, J. G. *J. Polym. Sci.* 1956, **22**, 79
23 Slichter, W. P. and Mandell, E. R. *J. Appl. Phys.* 1959, **30**, 1473
24 Tanaka, Y. and Ishida, Y. *J. Polym. Sci.* 1974, **12**, 335
25 Kashiwagi, M., Folkes, M. J. and Ward, I. M. *Polymer* 1971, **12**, 697
26 Tabka, M. T., Widmaier, J. M. and Meyer, G. C. *Macromolecules* 1989, **22**, 1826
27 Jin, S. R., Widmaier, J. M. and Meyer, G. C. *Polymer* 1988, **29**, 346